

Sensitivity and uncertainty analysis of β_{eff} for MYRRHA using a Monte Carlo technique

Hiroki Iwamoto^{1,2,*}, Alexey Stakovskiy¹, Luca Fiorito^{1,3}, and Gert Van den Eynde¹

¹ Institute for Advanced Nuclear Systems, Belgian Nuclear Research Centre (SCK-CEN), Boeretang 200, 2400 Mol, Belgium

² J-PARC Center, Japan Atomic Energy Agency (JAEA), 2-4, Shirakata, Tokai-mura, Naka-gun, Ibaraki 319-1195, Japan

³ Data Bank, OECD Nuclear Energy Agency (NEA), 46, Quai Alphonse Le Gallo 92100 Boulogne-Billancourt, France

Received: 3 October 2017 / Received in final form: 26 January 2018 / Accepted: 14 May 2018

Abstract. This paper presents a nuclear data sensitivity and uncertainty analysis of the effective delayed neutron fraction β_{eff} for critical and subcritical cores of the MYRRHA reactor using the continuous-energy Monte Carlo N-Particle transport code MCNP. The β_{eff} sensitivities are calculated by the modified k -ratio method proposed by Chiba. Comparing the β_{eff} sensitivities obtained with different scaling factors a introduced by Chiba shows that a value of $a = 20$ is the most suitable for the uncertainty quantification of β_{eff} . Using the calculated β_{eff} sensitivities and the JENDL-4.0u covariance data, the β_{eff} uncertainties for the critical and subcritical cores are determined to be $2.2 \pm 0.2\%$ and $2.0 \pm 0.2\%$, respectively, which are dominated by delayed neutron yield of ^{239}Pu and ^{238}U .

1 Introduction

To promote research and development of nuclear technology for various applications such as accelerator-driven systems, the Generation-IV reactors, and production of medical radioisotopes, the Belgian Nuclear Research Centre (SCK-CEN) has proposed a cutting-edge research reactor combined with a proton accelerator, MYRRHA [1,2]. From the viewpoint of ensuring safety margins and reducing uncertainty in the MYRRHA design parameters, uncertainty quantification of reactor physics parameters is one of the most important tasks. To this end, nuclear data sensitivity and uncertainty (S/U) analyses have been extensively conducted for various MYRRHA core configurations using different calculation tools, geometric models, and nuclear data libraries [3–5]; these works have focused on the effective neutron multiplication factor k_{eff} as the primary neutronic safety parameter. The effective delayed neutron fraction β_{eff} can be ranked second in the list of neutronic safety parameters, because, besides of reactor kinetics, it is used to determine other design and safety parameters such as control rod worth and Doppler coefficient.

Continuous-energy Monte Carlo transport codes such as the Monte Carlo N-Particle transport code MCNP [6] have been widely used in calculating not only k_{eff} but also

its nuclear data sensitivities and kinetic parameters including β_{eff} . Although these codes have no capability to directly calculate the β_{eff} sensitivities owing to technical cumbersomeness, it is approximately expressed as a function of two different k_{eff} sensitivities by the so-called “ k -ratio method [7]”; this indicates that uncertainty in β_{eff} can be quantified by the sensitivity method from the approximate β_{eff} sensitivities and evaluated covariance data of the nuclear data library. Although this method has been applied to the β_{eff} S/U analysis with a deterministic code SUS3D for MYRRHA in the studies of Kodeli [8], within the seventh framework programme solving Challenges in Nuclear DATA (CHANDA) project [9], the analysis using the Monte Carlo transport code has not yet been tackled.

The k -ratio method itself is currently subdivided into two techniques: the prompt k -ratio method [7] and the modified k -ratio method proposed by Chiba [10,11]. Our previous study [12] by MCNP for a critical configuration of the VENUS-F zero-power reactor at the SCK-CEN site [13] demonstrated that the prompt k -ratio method involves large statistical uncertainty in the calculated β_{eff} sensitivities, and it would be currently difficult to reduce it only by increasing the number of neutron source histories. On the other hand, we also demonstrated that Chiba’s modified k -ratio method can alleviate this kind of problem.

In this study, we conducted the S/U analysis of β_{eff} for two types of MYRRHA configurations (i.e. critical mode and subcritical mode) using Chiba’s modified k -ratio method. β_{eff} and its sensitivities were calculated using

* e-mail: iwamoto.hiroki@jaea.go.jp

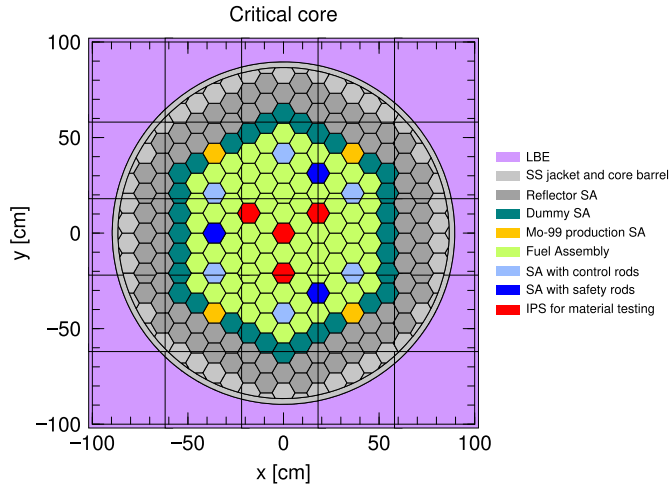


Fig. 1. Horizontal sectional view of MYRRHA critical core.

the MCNP version 6.1.1, and JENDL-4.0u [14,15] was used as the nuclear data library since it contains covariance data of delayed neutron yield $\bar{\nu}^d$.

2 MYRRHA core models

MYRRHA is designed to operate both in critical mode as a lead-bismuth cooled fast reactor and in subcritical mode driven by 600-MeV linear proton accelerator. Figures 1 and 2 show horizontal sectional views of the MYRRHA critical and subcritical configurations, respectively, which are homogenized on assembly level. The analyses were carried out for the critical and subcritical core configurations at beginning of cycle using the assembly-based homogenized models [16]. As illustrated, the critical and subcritical cores consist of 78 and 58 fuel assemblies (FAs), respectively; these are loaded with MOX with high Pu content. Besides FAs, the cores contains in-pile sections for material testing, irradiation rigs for medical isotope production, and subassemblies containing safety and control rods. More details of the MYRRHA core design are given in Van den Eynde et al. [2].

3 Methodology

3.1 The β_{eff} sensitivities

Chiba's modified k -ratio method describes β_{eff} as

$$\beta_{\text{eff}} \simeq \left(\frac{\bar{k}}{k} - 1 \right) \cdot \frac{1}{a}, \quad (1)$$

where $a (\neq 0)$ is a scaling factor; k is the effective multiplication factor calculated using the nuclear data library JENDL-4.0u; \bar{k} is the effective multiplication factor calculated using the library in which $\bar{\nu}^d$ is multiplied with $(a + 1)$ (Appendix A). If $a = -1$, then Chiba's modified k -

ratio method reduces to the prompt k -ratio method. The statistical uncertainty in β_{eff} propagated from δk and $\delta \bar{k}$ is expressed as follows:

$$\delta \beta_{\text{eff}} = \frac{\bar{k}}{k} \sqrt{\left(\frac{\delta \bar{k}}{\bar{k}} \right)^2 + \left(\frac{\delta k}{k} \right)^2} \cdot \frac{1}{|a|}. \quad (2)$$

Here correlations were disregarded for the sake of simplicity. Using the definition of the sensitivity and equation (1), the β_{eff} sensitivity to parameter x is expressed as follows:

$$S_x^{\beta_{\text{eff}}} \equiv \frac{\partial \beta_{\text{eff}}}{\partial x} \frac{x}{\beta_{\text{eff}}}, \quad (3)$$

$$\simeq \frac{\bar{k}}{\bar{k} - k} \left(S_x^{\bar{k}} - S_x^k \right), \quad (4)$$

where $S_x^k (\equiv (\partial k / \partial x) / (x/k))$ and $S_x^{\bar{k}} (\equiv (\partial \bar{k} / \partial x) / (x/\bar{k}))$ are the sensitivities of k and \bar{k} to the parameter x , respectively. The statistical uncertainty in $S_x^{\beta_{\text{eff}}}$ is expressed as

$$\delta S_x^{\beta_{\text{eff}}} \simeq |S_x^{\beta_{\text{eff}}}| \cdot \left\{ \left(\frac{\delta \bar{k}}{\bar{k}} \right)^2 + \frac{(\delta \bar{k})^2 + (\delta k)^2}{(\bar{k} - k)^2} + \frac{(\delta S_x^{\bar{k}})^2 + (\delta S_x^k)^2}{(S_x^{\bar{k}} - S_x^k)^2} \right\}^{1/2}, \quad (5)$$

where δS_x^k and $\delta S_x^{\bar{k}}$ are the statistical uncertainties in S_x^k and $S_x^{\bar{k}}$, respectively.

3.2 The β_{eff} uncertainties

Using the sensitivity profile obtained by the above-mentioned methods, the β_{eff} uncertainty (standard deviation) due to nuclear data was evaluated by the uncertainty propagation law considering covariance, which is expressed as

$$U^{\beta_{\text{eff}}} = \sqrt{\sum_z \sum_{z'} \sum_g \sum_{g'} S_{z,g}^{\beta_{\text{eff}}} \text{cov}(z, g; z', g') S_{z',g'}^{\beta_{\text{eff}}}}, \quad (6)$$

where $\text{cov}(z, g; z', g')$ denotes a $(g, g'; z, z')$ component of variance-covariance matrix (g, g' : energy group, z, z' : reaction), which was obtained by processing covariance data stored in JENDL-4.0u with NJOY [17] and ERRORJ [18]. In this analysis, we employed eight parameters: fission, neutron capture, elastic scattering, inelastic scattering, and $(n, 2n)$ reaction cross sections for major constituent materials: U, Pu, ^{241}Am , ^{16}O , ^{56}Fe , Pb, and ^{209}Bi , as well as prompt and delayed neutron yields and prompt neutron spectra for U and Pu isotopes. Here correlations between the reactions were also considered. Absence of covariance data for delayed neutron spectrum in JENDL-4.0u did not allow us to estimate the contribution to the β_{eff} and confirm the conclusion made by Kodeli [19] on its significance.

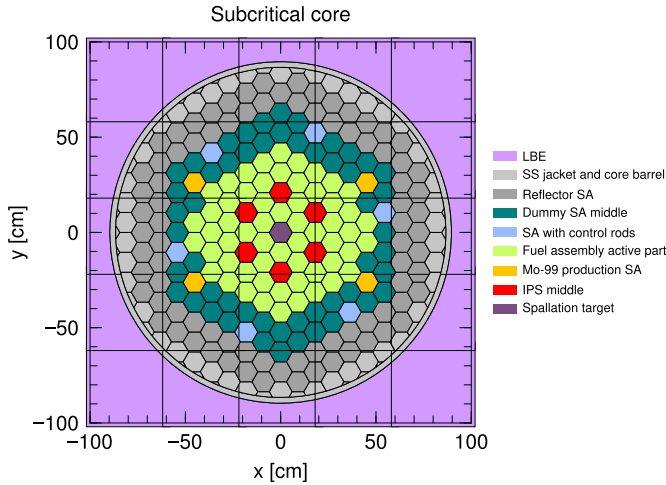


Fig. 2. Horizontal sectional view of MYRRHA subcritical core.

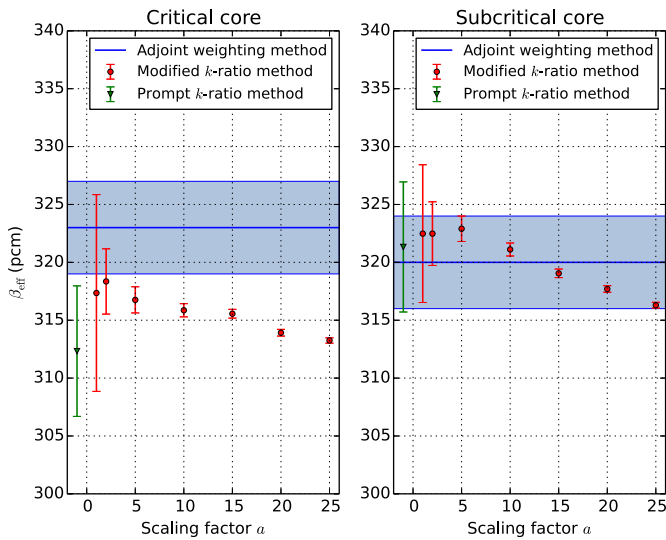


Fig. 3. Comparison of the β_{eff} values for different scaling factors calculated using Chiba's modified k -ratio method and that derived using the adjoint weighting method. The error bars and the band with pale blue color indicate 1σ statistical uncertainty.

4 Results and discussion

4.1 Effective delayed neutron fraction

Figure 3 shows comparisons of the calculated β_{eff} with different scaling factors ($a = -1, 1, 5, 10, 15, 20,$ and 25) for critical and subcritical cores. For each case, the k_{eff} value was calculated with 2.5×10^8 histories (2.5×10^5 source histories per cycle times 10^3 cycles) in the MCNP calculation flow. Here the value calculated directly by the adjoint weighting method [20] for the same number of histories for critical and subcritical cores were estimated to be 323 ± 4 and 320 ± 4 pcm, respectively. It can be seen that the calculated statistical uncertainty decreases with increase in a , which was about $|a|$ times smaller than that by the prompt k ratio method ($a = -1$). In addition, we see

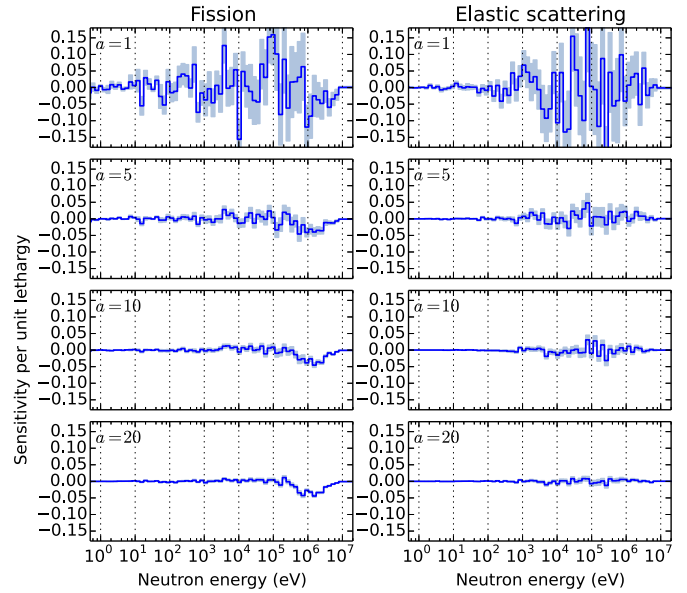


Fig. 4. Comparisons of β_{eff} sensitivity profile of ^{239}Pu fission (left) and elastic scattering (right) cross sections for the critical core with different scaling factors. The pale blue color around the blue line indicates 1σ statistical uncertainty.

that the calculated β_{eff} values exceeding their 1σ statistical uncertainties decrease as a increases. The similar trend can be seen in the previous study conducted for the VENUS-F reactor using MCNP [12] and the benchmark analysis for fast neutron systems conducted by Chiba using the deterministic transport code CBG [10,21]; this reason is linked to the approximation used in equation (1).

4.2 Sensitivity

Figures 4 and 5 show comparisons of the β_{eff} sensitivity profiles of ^{239}Pu fission and elastic scattering cross sections and ^{239}Pu $\bar{\nu}^p$ and $\bar{\nu}^d$ for the critical core with different scaling factors, respectively. As demonstrated in Iwamoto et al. [12], the statistical uncertainty at $a = 1$ is very large for all parameters except $\bar{\nu}^d$; this is caused by the small difference between S_x^k and S_x^k (Appendix A). In contrast, the statistical uncertainty for $\bar{\nu}^d$ is negligibly small for all the selected a values; this is owing to an approximation of $S_{\bar{\nu}^d}^k \simeq (a+1)S_{\bar{\nu}^d}^k$ (Appendix A). In addition, as with the β_{eff} values, $\delta S_x^{\beta_{\text{eff}}}$ decrease as a increases. However, it should be noted that the β_{eff} sensitivities change within about 1σ statistical uncertainties, while the nominal values of β_{eff} tend to exceed their 1σ statistical uncertainties. This indicates that the influence of the change in the β_{eff} sensitivities that results from increasing a on the uncertainty quantification of β_{eff} is expected to be small.

Figures 6 and 7 show the β_{eff} sensitivity profiles with respect to ^{239}Pu and ^{238}U reaction parameters for the critical core with $a = 20$, respectively, in which the statistical uncertainties appear to be sufficiently small. Table 1 summarizes the major β_{eff} sensitivities together with 1σ statistical uncertainties which were calculated with $a = 20$. As expected from the definition of β_{eff} , $\bar{\nu}^d$ of major

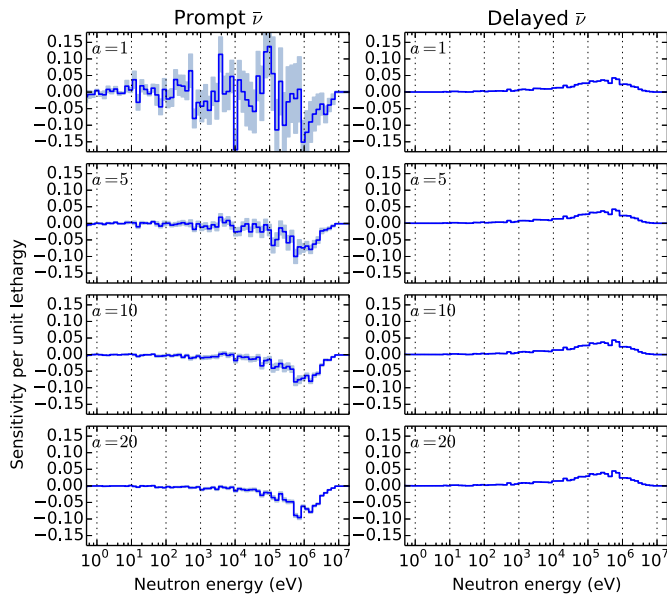


Fig. 5. Comparisons of β_{eff} sensitivity profile of ^{239}Pu $\bar{\nu}^p$ (left) and $\bar{\nu}^d$ (right) for the critical core with different scaling factors. The pale blue color around the blue line indicates 1σ statistical uncertainty.

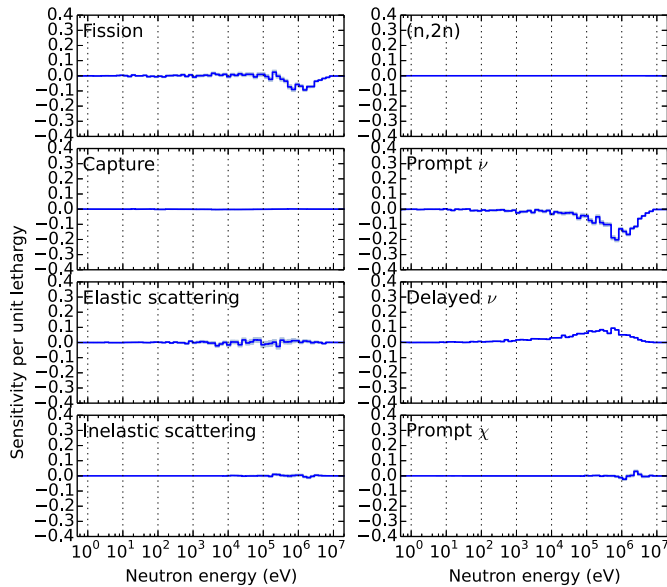


Fig. 6. ^{239}Pu sensitivity profile for the critical core ($a=20$).

fuel materials (i.e. ^{239}Pu and ^{238}U) shows positive high sensitivities; in contrast, $\bar{\nu}^p$ demonstrates negative sensitivities.

4.3 Uncertainty

Table 2 lists the β_{eff} uncertainties due to nuclear data with different scaling factors for the critical and subcritical cores. Small scaling factors produce large both uncertainty values and their statistical uncertainties. This arises from

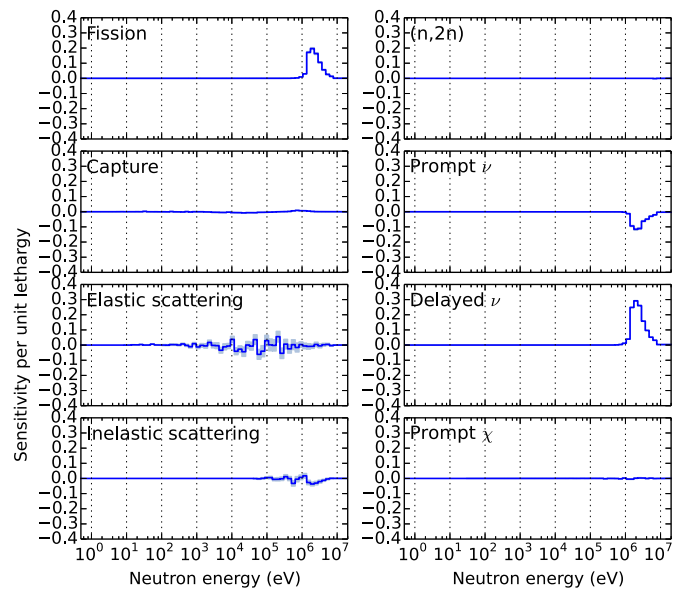


Fig. 7. ^{238}U sensitivity profile for the critical core ($a=20$).

the large sensitivities with large statistical uncertainties in the sensitivity profile as mentioned above; these statistical uncertainties can be reduced by increasing a . In addition, we see from Table 2 that, as a increases, the calculated total β_{eff} uncertainties for the critical and subcritical cores approach values of 2.2% and 2.0%, respectively.

Table 3 summarizes top 15 contributors to the β_{eff} uncertainty together with 1σ statistical uncertainties. Overall, the statistical uncertainties are small enough to identify the main contributors; namely, it can be concluded that the β_{eff} uncertainty is dominated by $\bar{\nu}^d$, followed by the elastic and inelastic scattering cross sections, for both cores.

5 Conclusion

We have conducted the nuclear data S/U analysis of β_{eff} for critical and subcritical cores of the MYRRHA reactor using the MCNP code. The β_{eff} sensitivities were calculated by Chiba's modified k -ratio method. Although the nominal β_{eff} values appear to worsen as a increases, comparing the β_{eff} sensitivities and their statistical uncertainties calculated with different scaling factors shows that the β_{eff} sensitivities are more stable to the a change than the nominal β_{eff} values, and that a value of $a=20$ is the most suitable for the uncertainty quantification. Using the calculated β_{eff} sensitivities and the JENDL-4.0u covariance data, the β_{eff} uncertainties for the critical and subcritical cores have been determined to be $2.2 \pm 0.2\%$ and $2.0 \pm 0.2\%$, respectively, which are dominated by $\bar{\nu}^d$ of ^{239}Pu and ^{238}U .

To account for the optimal a value more clearly, further investigation, especially for non-linear effects on $\bar{\psi}_a$ and $\bar{\psi}_a^{-1}$, is needed. Moreover, it would be of interest to compare our results with those previously performed using the deterministic code within the ongoing CHANDA project [8].

Table 1. Major β_{eff} sensitivities with 1σ statistical uncertainties ($a = 20$, top 15).

Nuclide	Reaction	Sensitivity (%/%)	
		Critical core	Subcritical core
^{239}Pu	$\bar{\nu}^p$	-0.589 ± 0.013	-0.520 ± 0.011
^{239}Pu	$\bar{\nu}^d$	0.409 ± 0.001	0.362 ± 0.001
^{238}U	$\bar{\nu}^d$	0.303 ± 0.001	0.277 ± 0.001
^{238}U	Fission	0.195 ± 0.003	0.175 ± 0.003
^{239}Pu	Fission	-0.154 ± 0.013	-0.140 ± 0.012
^{241}Pu	$\bar{\nu}^d$	0.136 ± 0.000	0.119 ± 0.000
^{238}U	$\bar{\nu}^p$	-0.128 ± 0.003	-0.119 ± 0.002
^{240}Pu	$\bar{\nu}^p$	-0.114 ± 0.002	-0.105 ± 0.002
^{241}Pu	Fission	0.070 ± 0.002	0.060 ± 0.002
^{241}Pu	$\bar{\nu}^p$	-0.067 ± 0.002	-0.057 ± 0.002
^{240}Pu	$\bar{\nu}^d$	0.063 ± 0.000	0.057 ± 0.000
^{238}U	Elastic	-0.049 ± 0.037	0.006 ± 0.032
^{56}Fe	Elastic	-0.037 ± 0.037	-0.058 ± 0.032
^{240}Pu	Fission	-0.036 ± 0.002	-0.035 ± 0.002
^{238}U	Inelastic	-0.034 ± 0.013	-0.019 ± 0.011

Table 2. Calculated β_{eff} uncertainty with different scaling factors.

a	Uncertainty (%)	
	Critical core	Subcritical core
-1	9.3 ± 3.0	7.6 ± 2.5
1	8.7 ± 4.6	2.7 ± 1.4
2	4.5 ± 1.9	2.1 ± 0.9
5	2.7 ± 0.6	1.9 ± 0.4
10	2.3 ± 0.5	1.9 ± 0.4
15	2.2 ± 0.3	1.9 ± 0.2
20	2.2 ± 0.2	2.0 ± 0.2

Table 3. Major contributors to the β_{eff} uncertainty with 1σ statistical uncertainties ($a = 20$, top 15).

Nuclide	Reaction	Uncertainty (%)	
		Critical core	Subcritical core
^{239}Pu	$\bar{\nu}^d$	1.683 ± 0.000	1.496 ± 0.000
^{238}U	$\bar{\nu}^d$	1.022 ± 0.001	0.908 ± 0.001
^{241}Pu	$\bar{\nu}^d$	0.677 ± 0.000	0.602 ± 0.000
^{238}U	Inelastic	0.389 ± 0.044	0.345 ± 0.039
^{240}Pu	$\bar{\nu}^d$	0.307 ± 0.000	0.273 ± 0.000
^{56}Fe	Elastic	0.274 ± 0.078	0.244 ± 0.069
^{242}Pu	$\bar{\nu}^d$	0.215 ± 0.000	0.192 ± 0.000
^{56}Fe	Inelastic	0.189 ± 0.046	0.168 ± 0.041
^{206}Pb	Inelastic	0.170 ± 0.019	0.151 ± 0.017
^{206}Pb	Elastic	0.136 ± 0.044	0.120 ± 0.039
^{208}Pb	Elastic	0.128 ± 0.042	0.114 ± 0.037
^{238}U	Elastic	0.128 ± 0.166	0.113 ± 0.147
^{238}U	Fission	0.115 ± 0.001	0.103 ± 0.001
^{239}Pu	Fission	0.103 ± 0.002	0.091 ± 0.001
^{239}Pu	Inelastic	0.099 ± 0.026	0.088 ± 0.023
Total		2.2 ± 0.2	2.0 ± 0.2

Appendix A: Chiba's modified k -ratio method

In equation (1), the effective neutron multiplication factor k_{eff} is obtained by solving the following neutron transport equation:

$$(\mathcal{T} - \mathcal{S})\psi = \frac{1}{k}\mathcal{F}\psi, \quad (\text{A.1})$$

where $\psi(= \psi(\mathbf{r}, \mathbf{\Omega}, E))$ is the angular neutron flux at position \mathbf{r} with direction $\mathbf{\Omega}$ and energy E ; \mathcal{T} , \mathcal{S} , and \mathcal{F} are the transport, scattering, and fission operators, respectively, which are expressed as follows:

$$\mathcal{T} = \mathbf{\Omega} \cdot \nabla + \Sigma_t(\mathbf{r}, E), \quad (\text{A.2})$$

$$\mathcal{S} = \int d\mathbf{\Omega}' \int dE' \Sigma_s(\mathbf{r}, \mathbf{\Omega}, E \leftarrow \mathbf{\Omega}', E'),$$

$$\mathcal{F} = \int d\mathbf{\Omega}' \int dE' \chi(\mathbf{\Omega}, E) \bar{\nu}(E') \Sigma_f(\mathbf{r}, E'). \quad (\text{A.4})$$

Here Σ_t , Σ_s , and Σ_f represent the macroscopic total, scattering, and fission cross sections, respectively; χ and $\bar{\nu}$ are total fission neutron spectrum and fission neutron yield, respectively. The effective multiplication factor \bar{k} in equation (1) is obtained by solving a fictitious neutron transport equation below:

$$(\mathcal{T} - \mathcal{S})\bar{\psi}_a = \frac{1}{\bar{k}}\bar{\mathcal{F}}_a\bar{\psi}_a, \quad (\text{A.5})$$

where $\bar{\psi}_a$ is the fictitious angular neutron flux obtained from equation (A.5); $\bar{\mathcal{F}}_a$ is a fission operator defined as follows:

$$\begin{aligned} \bar{\mathcal{F}}_a = & \int d\mathbf{\Omega}' \int dE' (\chi(\mathbf{\Omega}, E) \bar{\nu}(E') \\ & + a\chi^d(\mathbf{\Omega}, E) \bar{\nu}^d(E')) \Sigma_f(\mathbf{r}, E'). \end{aligned} \quad (\text{A.6})$$

Using the relationship between prompt, delayed, and total neutrons:

$$\chi\bar{\nu} = \chi^p\bar{\nu}^p + \chi^d\bar{\nu}^d. \quad (\text{A.7})$$

Equation (A.6) can be rewritten as

$$\begin{aligned} \bar{\mathcal{F}}_a = & \int d\mathbf{\Omega}' \int dE' (\chi^p(\mathbf{\Omega}, E) \bar{\nu}^p(E') \\ & + (a+1)\chi^d(\mathbf{\Omega}, E) \bar{\nu}^d(E')) \Sigma_f(\mathbf{r}, E'). \end{aligned} \quad (\text{A.8})$$

It is noted that a corresponds to the fractional change of $\bar{\nu}^d$ and that, if $a = -1$ is adopted, only prompt neutrons are taken into account; in this case, Chiba's modified k -ratio method reduces to the prompt k -ratio method [22]. In the MCNP calculation, \bar{k} is obtained using a nuclear data library in which $\bar{\nu}^d$ is multiplied with $(a+1)$.

According to the adjoint-based perturbation theory, the sensitivity of k to parameter x is expressed as [23]

$$S_x^k = - \frac{\langle \psi^\dagger, (\Sigma_x - \mathcal{S}_x - \lambda\mathcal{F}_x)\psi \rangle}{\langle \psi^\dagger, \lambda\mathcal{F}\psi \rangle}, \quad (\text{A.9})$$

where the bracket \langle, \rangle represents integration over the phase space; ψ^\dagger is the adjoint function of ψ ; $\lambda = 1/k$; Σ_x is the macroscopic cross section corresponding to parameter x ; \mathcal{S}_x is the scattering operator for parameter x ; \mathcal{F}_x is the fission operator for parameter x .

As an example of parameters except for $\bar{\nu}^d$, let us consider neutron capture cross section σ_{cap} . Since σ_{cap} involves neither scattering nor fission, the sensitivity of k to σ_{cap} is written by

$$S_{\sigma_{\text{cap}}}^k = - \frac{\langle \psi^\dagger, \Sigma_{\text{cap}}\psi \rangle}{\langle \psi^\dagger, \lambda\mathcal{F}\psi \rangle}. \quad (\text{A.10})$$

Further, the sensitivity of \bar{k} to σ_{cap} is written by

$$S_{\sigma_{\text{cap}}}^{\bar{k}} = - \frac{\langle \bar{\psi}_a^\dagger, \Sigma_{\text{cap}}\bar{\psi}_a \rangle}{\langle \bar{\psi}_a^\dagger, \bar{\lambda}\bar{\mathcal{F}}_a\bar{\psi}_a \rangle}, \quad (\text{A.11})$$

where $\bar{\lambda} = 1/\bar{k}$ and Σ_{cap} represents the macroscopic capture cross section. We see from equation (A.6) that, if a approaches zero, $\bar{\mathcal{F}}_a$ becomes \mathcal{F} ; and hence $\bar{\psi}_a$, $\bar{\psi}_a^\dagger$, and \bar{k} become ψ , ψ^\dagger , and k , respectively. Namely, if a small value is chosen for a , the difference between equations (A.10) and (A.11) is also small.

Similarly, the sensitivities of k and k to $\bar{\nu}^d$ are written by

$$S_{\bar{\nu}^d}^k = \frac{\langle \psi^\dagger, \mathcal{F}_{\bar{\nu}^d}\psi \rangle}{\langle \psi^\dagger, \mathcal{F}\psi \rangle}, \quad (\text{A.12})$$

and

$$S_{\bar{\nu}^d}^{\bar{k}} = \frac{\langle \bar{\psi}_a^\dagger, \bar{\mathcal{F}}_{a, \bar{\nu}^d}\bar{\psi}_a \rangle}{\langle \bar{\psi}_a^\dagger, \bar{\mathcal{F}}_a\bar{\psi}_a \rangle} = (a+1) \frac{\langle \bar{\psi}_a^\dagger, \mathcal{F}_{\bar{\nu}^d}\bar{\psi}_a \rangle}{\langle \bar{\psi}_a^\dagger, \bar{\mathcal{F}}_a\bar{\psi}_a \rangle}, \quad (\text{A.13})$$

respectively. As with the case of other parameters, as a approaches zero, the limit of equation (A.13) of a equals equation (A.12). If a particular value is chosen for a to the extent that the approximations of $\mathcal{F} \simeq \bar{\mathcal{F}}_a$, $\psi \simeq \bar{\psi}_a$, and $\psi^\dagger \simeq \bar{\psi}_a^\dagger$ are applicable, equation (A.13) can be expressed as follows:

$$S_{\bar{\nu}^d}^{\bar{k}} \simeq (a+1)S_{\bar{\nu}^d}^k. \quad (\text{A.14})$$

Thus, if $a = 1$ is used, then $S_{\bar{\nu}^d}^{\bar{k}}$ is about twice as large as $S_{\bar{\nu}^d}^k$; namely, it follows that there is a large difference between the two.

References

1. H.A. Abderrahim et al., *Energy Convers. Manag.* **63**, 4 (2012)
2. G. Van den Eynde et al., *J. Nucl. Sci. Technol.* **52**, 1053 (2015)
3. T. Sugawara et al., *Ann. Nucl. Energy* **38**, 1098 (2011)
4. C.J. Diez et al., *Nucl. Data Sheets* **118**, 516 (2014)
5. P. Romojaro et al., *Ann. Nucl. Energy* **101**, 330 (2017)
6. J.T. Goorley, LA-UR-14-24680, 2014
7. M.M. Bretscher, in *Proceedings of the International Meeting on Reduced Enrichment for Research and Test Reactors, Jackson Hole* (1997)
8. I. Kodeli, *Ann. Nucl. Energy* **113**, 425 (2018)
9. CHANDA Project, EC Community Research and Development Information Service, <http://www.chanda-nd.eu>
10. G. Chiba, *J. Nucl. Sci. Technol.* **46**, 399 (2009)
11. G. Chiba et al., *J. Nucl. Sci. Technol.* **48**, 1471 (2011)
12. H. Iwamoto et al., *J. Nucl. Sci. Technol.* **55**, 539 (2018)
13. X. Doligez et al., in *Proceedings of the 2015 4th International Conference on Advancements in Nuclear Instrumentation Measurement Methods and their Applications (ANIMMA 2015), Lisbon* (2016)
14. K. Shibata et al., *J. Nucl. Sci. Technol.* **48**, 1 (2011)
15. O. Iwamoto et al., *J. Korean Phys. Soc.* **59**, 1224 (2011)
16. A. Stankovskiy, G. Van den Eynde, SCK-CEN/4463803, 2014
17. R.E. MacFarlane et al., LA-UR-12-2079 Rev, 2012
18. G. Chiba, JAEA-Data/Code2007-007, 2007
19. I. Kodeli, *Nucl. Instr. Meth. Phys. Res. A* **715**, 70 (2013)
20. B. Kiedrowski, F. Brown, LA-UR-09-02594, 2009
21. G. Chiba, JAEA-Research 2009-012, 2009
22. Y. Nagaya, T. Mori, *Ann. Nucl. Energy* **38**, 254 (2011)
23. B. Kiedrowski, LA-UR-13-24254, 2013

Cite this article as: Hiroki Iwamoto, Alexey Stakovskiy, Luca Fiorito, Gert Van den Eynde, Sensitivity and uncertainty analysis of β_{eff} for MYRRHA using a Monte Carlo technique, *EPJ Nuclear Sci. Technol.* **4**, 42 (2018)